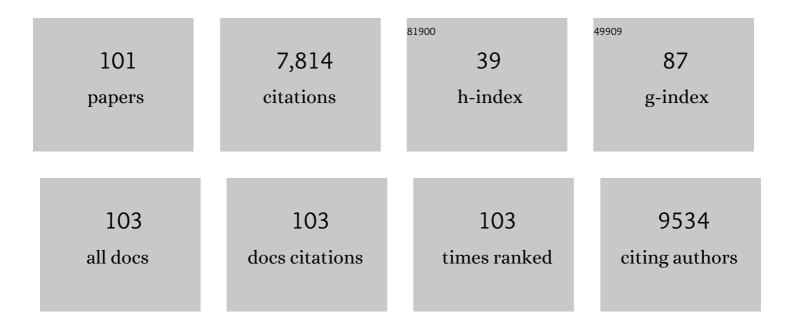
List of Publications by Year in descending order

Source: https://exaly.com/author-pdf/6533578/publications.pdf Version: 2024-02-01



KALCHEN

#	Article	IF	CITATIONS
1	In vivo biodistribution and highly efficient tumour targeting of carbon nanotubes in mice. Nature Nanotechnology, 2007, 2, 47-52.	31.5	1,384
2	PET/MRI Dual-Modality Tumor Imaging Using Arginine-Glycine-Aspartic (RGD)–Conjugated Radiolabeled Iron Oxide Nanoparticles. Journal of Nuclear Medicine, 2008, 49, 1371-1379.	5.0	507
3	PET/NIRF/MRI triple functional iron oxide nanoparticles. Biomaterials, 2010, 31, 3016-3022.	11.4	456
4	Dual-Function Probe for PET and Near-Infrared Fluorescence Imaging of Tumor Vasculature. Journal of Nuclear Medicine, 2007, 48, 1862-1870.	5.0	400
5	Albumin/vaccine nanocomplexes that assemble in vivo for combination cancer immunotherapy. Nature Communications, 2017, 8, 1954.	12.8	237
6	Quantitative PET of EGFR expression in xenograft-bearing mice using 64Cu-labeled cetuximab, a chimeric anti-EGFR monoclonal antibody. European Journal of Nuclear Medicine and Molecular Imaging, 2007, 34, 850-858.	6.4	231
7	64Cu-Labeled Tetrameric and Octameric RGD Peptides for Small-Animal PET of Tumor ÂvÂ3 Integrin Expression. Journal of Nuclear Medicine, 2007, 48, 1162-1171.	5.0	227
8	Integrin Targeted Delivery of Chemotherapeutics. Theranostics, 2011, 1, 189-200.	10.0	203
9	Radiolabeled Nanoparticles for Multimodality Tumor Imaging. Theranostics, 2014, 4, 290-306.	10.0	201
10	ln vitro and In vivo Characterization of 64Cu-Labeled AbegrinTM, a Humanized Monoclonal Antibody against Integrin αvβ3. Cancer Research, 2006, 66, 9673-9681.	0.9	192
11	68Ga-labeled multimeric RGD peptides for microPET imaging of integrin αvβ3 expression. European Journal of Nuclear Medicine and Molecular Imaging, 2008, 35, 1100-1108.	6.4	192
12	Dual-modality optical and positron emission tomography imaging of vascular endothelial growth factor receptor on tumor vasculature using quantum dots. European Journal of Nuclear Medicine and Molecular Imaging, 2008, 35, 2235-2244.	6.4	189
13	Design and Development of Molecular Imaging Probes. Current Topics in Medicinal Chemistry, 2010, 10, 1227-1236.	2.1	174
14	Target-specific delivery of peptide-based probes for PET imaging. Advanced Drug Delivery Reviews, 2010, 62, 1005-1022.	13.7	161
15	Triblock copolymer coated iron oxide nanoparticle conjugate for tumor integrin targeting. Biomaterials, 2009, 30, 6912-6919.	11.4	147
16	Transformative Nanomedicine of an Amphiphilic Camptothecin Prodrug for Long Circulation and High Tumor Uptake in Cancer Therapy. ACS Nano, 2017, 11, 8838-8848.	14.6	144
17	Click Chemistry for <sup>18</sup> F-Labeling of RGD Peptides and microPET Imaging of Tumor Integrin α <sub>v</sub> β <sub>3</sub> Expression. Bioconjugate Chemistry, 2007, 18, 1987-1994.	3.6	139
18	<sup>18</sup> F-Labeled BBN-RGD Heterodimer for Prostate Cancer Imaging. Journal of Nuclear Medicine, 2008, 49, 453-461.	5.0	132

#	Article	IF	CITATIONS
19	18F-Labeled Galacto and PEGylated RGD Dimers for PET Imaging of αvβ3 Integrin Expression. Molecular Imaging and Biology, 2010, 12, 530-538.	2.6	131
20	microPET of Tumor Integrin ÂvÂ3 Expression Using 18F-Labeled PEGylated Tetrameric RGD Peptide (18F-FPRGD4). Journal of Nuclear Medicine, 2007, 48, 1536-1544.	5.0	120
21	A new PET tracer specific for vascular endothelial growth factor receptor 2. European Journal of Nuclear Medicine and Molecular Imaging, 2007, 34, 2001-2010.	6.4	114
22	Imaging of VEGF Receptor in a Rat Myocardial Infarction Model Using PET. Journal of Nuclear Medicine, 2008, 49, 667-673.	5.0	102
23	Positron Emission Tomography Imaging of Cancer Biology: Current Status and Future Prospects. Seminars in Oncology, 2011, 38, 70-86.	2.2	98
24	Multimodality molecular imaging of glioblastoma growth inhibition with vasculature-targeting fusion toxin VEGF121/rGel. Journal of Nuclear Medicine, 2007, 48, 445-54.	5.0	85
25	<sup>18</sup> F-Labeled GRPR Agonists and Antagonists: A Comparative Study in Prostate Cancer Imaging. Theranostics, 2011, 1, 220-229.	10.0	73
26	Evaluation of biodistribution and anti-tumor effect of a dimeric RGD peptide–paclitaxel conjugate in mice with breast cancer. European Journal of Nuclear Medicine and Molecular Imaging, 2008, 35, 1489-1498.	6.4	71
27	Quantitative PET Imaging of VEGF Receptor Expression. Molecular Imaging and Biology, 2009, 11, 15-22.	2.6	71
28	Synthesis and Evaluation of <sup>64</sup> Cu-Labeled Monomeric and Dimeric NGR Peptides for MicroPET Imaging of CD13 Receptor Expression. Molecular Pharmaceutics, 2013, 10, 417-427.	4.6	64
29	Pretargeted Positron Emission Tomography Imaging That Employs Supramolecular Nanoparticles with <i>in Vivo</i> Bioorthogonal Chemistry. ACS Nano, 2016, 10, 1417-1424.	14.6	60
30	Polyethyleneimine-Coated Manganese Oxide Nanoparticles for Targeted Tumor PET/MR Imaging. ACS Applied Materials & Interfaces, 2018, 10, 34954-34964.	8.0	56
31	Integrin-targeted imaging and therapy with RGD4C-TNF fusion protein. Molecular Cancer Therapeutics, 2008, 7, 1044-1053.	4.1	53
32	Boramino acid as a marker for amino acid transporters. Science Advances, 2015, 1, e1500694.	10.3	49
33	In silico design, synthesis, and biological evaluation of radioiodinated quinazolinone derivatives for alkaline phosphatase–mediated cancer diagnosis and therapy. Molecular Cancer Therapeutics, 2006, 5, 3001-3013.	4.1	47
34	MicroPET Imaging of CD13 Expression Using a <sup>64</sup> Cu-Labeled Dimeric NGR Peptide Based on Sarcophagine Cage. Molecular Pharmaceutics, 2014, 11, 3938-3946.	4.6	47
35	Recent advances in the development of nanoparticles for multimodality imaging and therapy of cancer. Medicinal Research Reviews, 2020, 40, 909-930.	10.5	46
36	A new 18F-labeled BBN-RGD peptide heterodimer with a symmetric linker for prostate cancer imaging. Amino Acids, 2011, 41, 439-447.	2.7	45

#	Article	IF	CITATIONS
37	Evaluation of 64Cu Labeled GX1: A Phage Display Peptide Probe for PET Imaging of Tumor Vasculature. Molecular Imaging and Biology, 2012, 14, 96-105.	2.6	43
38	Small molecules as theranostic agents in cancer immunology. Theranostics, 2019, 9, 7849-7871.	10.0	42
39	Non-Invasive PET Imaging of EGFR Degradation Induced by a Heat Shock Protein 90 Inhibitor. Molecular Imaging and Biology, 2008, 10, 99-106.	2.6	41
40	A Cy5.5-labeled phage-displayed peptide probe for near-infrared fluorescence imaging of tumor vasculature in living mice. Amino Acids, 2012, 42, 1329-1337.	2.7	39
41	Strain-Promoted Catalyst-Free Click Chemistry for Rapid Construction of <sup>64</sup> Cu-Labeled PET Imaging Probes. ACS Medicinal Chemistry Letters, 2012, 3, 1019-1023.	2.8	38
42	64Cu-Labeled multifunctional dendrimers for targeted tumor PET imaging. Nanoscale, 2018, 10, 6113-6124.	5.6	38
43	PET imaging of early response to the tyrosine kinase inhibitor ZD4190. European Journal of Nuclear Medicine and Molecular Imaging, 2011, 38, 1237-1247.	6.4	37
44	Phage Display–Derived Peptides for Osteosarcoma Imaging. Clinical Cancer Research, 2010, 16, 4268-4277.	7.0	36
45	Macrophages as a potential tumor-microenvironment target for noninvasive imaging of early response to anticancer therapy. Biomaterials, 2018, 152, 63-76.	11.4	36
46	Design of Targeted Cardiovascular Molecular Imaging Probes. Journal of Nuclear Medicine, 2010, 51, 3S-17S.	5.0	35
47	99mTc-labeled monomeric and dimeric NGR peptides for SPECT imaging of CD13 receptor in tumor-bearing mice. Amino Acids, 2013, 44, 1337-1345.	2.7	35
48	Molecular-Docking-Guided Design, Synthesis, and Biologic Evaluation of Radioiodinated Quinazolinone Prodrugs. Journal of Medicinal Chemistry, 2007, 50, 663-673.	6.4	34
49	64Cu-Labeled PEGylated Polyethylenimine for Cell Trafficking and Tumor Imaging. Molecular Imaging and Biology, 2009, 11, 415-423.	2.6	30
50	Synthesis and Biologic Evaluation of a Radioiodinated Quinazolinone Derivative for Enzyme-Mediated Insolubilization Therapy. Bioconjugate Chemistry, 2002, 13, 357-364.	3.6	29
51	Using Hoechst 33342 to Target Radioactivity to the Cell Nucleus. Radiation Research, 2007, 167, 167-175.	1.5	29
52	Near-infrared fluorescence imaging of CD13 receptor expression using a novel Cy5.5-labeled dimeric NGR peptide. Amino Acids, 2014, 46, 1547-1556.	2.7	27
53	Near-Infrared Hybrid Rhodol Dyes with Spiropyran Switches for Sensitive Ratiometric Sensing of pH Changes in Mitochondria and <i>Drosophila melanogaster</i> First-Instar Larvae. ACS Applied Bio Materials, 2019, 2, 4986-4997.	4.6	27
54	68Ga-Labeled Cyclic NGR Peptide for MicroPET Imaging of CD13 Receptor Expression. Molecules, 2014, 19, 11600-11612.	3.8	26

#	Article	IF	CITATIONS
55	Recent advances in diagnosis and treatment of gliomas using chlorotoxin-based bioconjugates. American Journal of Nuclear Medicine and Molecular Imaging, 2014, 4, 385-405.	1.0	26
56	Molecular modeling of the interaction of iodinated Hoechst analogs with DNA: implications for new radiopharmaceutical design. Computational and Theoretical Chemistry, 2004, 711, 49-56.	1.5	25
57	Auger Electron-Induced Double-Strand Breaks Depend on DNA Topology. Radiation Research, 2008, 170, 70-82.	1.5	25
58	A direct comparison of tumor angiogenesis with 68Ga-labeled NGR and RGD peptides in HT-1080 tumor xenografts using microPET imaging. Amino Acids, 2014, 46, 2355-2364.	2.7	25
59	Supramolecular nanosubstrate–mediated delivery system enables CRISPR-Cas9 knockin of hemoglobin beta gene for hemoglobinopathies. Science Advances, 2020, 6, .	10.3	25
60	Design, synthesis and validation of integrin α2β1-targeted probe for microPET imaging of prostate cancer. European Journal of Nuclear Medicine and Molecular Imaging, 2011, 38, 1313-1322.	6.4	22
61	Mechanisms Underlying Production of Double-Strand Breaks in Plasmid DNA after Decay of1251-Hoechst. Radiation Research, 2006, 166, 333-344.	1.5	19
62	Cross-Linked Fluorescent Supramolecular Nanoparticles for Intradermal Controlled Release of Antifungal Drug—A Therapeutic Approach for Onychomycosis. ACS Nano, 2018, 12, 6851-6859.	14.6	19
63	RGD-human serum albumin conjugates as efficient tumor targeting probes. Molecular Imaging, 2009, 8, 65-73.	1.4	18
64	Phage display peptide probes for imaging early response to bevacizumab treatment. Amino Acids, 2011, 41, 1103-1112.	2.7	17
65	Development of PET Probes for Cancer Imaging. Current Topics in Medicinal Chemistry, 2015, 15, 795-819.	2.1	17
66	Understanding the Exchange of Systemic HDL Particles Into the Brain and Vascular Cells Has Diagnostic and Therapeutic Implications for Neurodegenerative Diseases. Frontiers in Physiology, 2021, 12, 700847.	2.8	16
67	Molecular Simulation of Ligandâ€Binding with DNA: Implications for125I‣abeled Pharmaceutical Design. International Journal of Radiation Biology, 2004, 80, 921-926.	1.8	15
68	Recent advances and applications of microspheres and nanoparticles in transarterial chemoembolization for hepatocellular carcinoma. Wiley Interdisciplinary Reviews: Nanomedicine and Nanobiotechnology, 2022, 14, e1749.	6.1	15
69	Synthesis of Coumarin–Polyamine-Based Molecular Probe for the Detection of Hydroxyl Radicals Generated by Gamma Radiation. Radiation Research, 2007, 168, 233-242.	1.5	14
70	Radiofluorinated GPC3-Binding Peptides for PET Imaging of Hepatocellular Carcinoma. Molecular Imaging and Biology, 2020, 22, 134-143.	2.6	14
71	In vivo NIRF imaging-guided delivery of a novel NGR–VEGI fusion protein for targeting tumor vasculature. Amino Acids, 2014, 46, 2721-2732.	2.7	13
72	[ <sup>18</sup> F]-2′ -Fluoro-5-methyl-1-beta-D-arabinofuranosyluracil ( <sup>18</sup> F-FMAU) in Prostate Cancer: Initial Preclinical Observations. Molecular Imaging, 2012, 11, 7290.2012.00004.	1.4	12

#	Article	IF	CITATIONS
73	Phosphoproteomics reveals ALK promote cell progress via RAS/JNK pathway in neuroblastoma. Oncotarget, 2016, 7, 75968-75980.	1.8	12
74	Prp19 Is an Independent Prognostic Marker and Promotes Neuroblastoma Metastasis by Regulating the Hippo-YAP Signaling Pathway. Frontiers in Oncology, 2020, 10, 575366.	2.8	12
75	XPO1/CRM1 is a promising prognostic indicator for neuroblastoma and represented a therapeutic target by selective inhibitor verdinexor. Journal of Experimental and Clinical Cancer Research, 2021, 40, 255.	8.6	12
76	PCLAF promotes neuroblastoma G1/S cell cycle progression via the E2F1/PTTG1 axis. Cell Death and Disease, 2022, 13, 178.	6.3	12
77	Targeted Prostate Gland Biopsy With Combined Transrectal Ultrasound, mpMRI, and 18F-FMAU PET/CT. Clinical Nuclear Medicine, 2015, 40, e426-e428.	1.3	11
78	Evaluation of 188Re-labeled NGR–VEGI protein for radioimaging and radiotherapy in mice bearing human fibrosarcoma HT-1080 xenografts. Tumor Biology, 2016, 37, 9121-9129.	1.8	11
79	Cross-Linked Fluorescent Supramolecular Nanoparticles as Finite Tattoo Pigments with Controllable Intradermal Retention Times. ACS Nano, 2017, 11, 153-162.	14.6	11
80	MCM6 indicates adverse tumor features and poor outcomes and promotes G1/S cell cycle progression in neuroblastoma. BMC Cancer, 2021, 21, 784.	2.6	11
81	Both serum and tissue Galectinâ€l levels are associated with adverse clinical features in neuroblastoma. Pediatric Blood and Cancer, 2018, 65, e27229.	1.5	10
82	Molecular Imaging of Tumor Microenvironment to Assess the Effects of Locoregional Treatment for Hepatocellular Carcinoma. Hepatology Communications, 2022, 6, 652-664.	4.3	10
83	Recent Progress in Lymphangioma. Frontiers in Pediatrics, 2021, 9, 735832.	1.9	10
84	MYT1 attenuates neuroblastoma cell differentiation by interacting with the LSD1/CoREST complex. Oncogene, 2020, 39, 4212-4226.	5.9	9
85	[18F]-2'-Fluoro-5-methyl-1-beta-D-arabinofuranosyluracil (18F-FMAU) in prostate cancer: initial preclinical observations. Molecular Imaging, 2012, 11, 426-32.	1.4	9
86	Microwave-assisted one-pot radiosynthesis of 2′-deoxy-2′-[18F]fluoro-5-methyl-1-β-d-arabinofuranosyluracil ([18F]-FMAU). Nuclear Medicine and Biology, 2012, 39, 1019-1025.	0.6	8
87	PET imaging of Hsp90 expression in pancreatic cancer using a new 64Cu-labeled dimeric Sansalvamide A decapeptide. Amino Acids, 2018, 50, 897-907.	2.7	8
88	A comparison of the monomeric [68Ga]NODAGA-NGR and dimeric [68Ga]NOTA-(NGR)2 as aminopeptidase N ligand for positron emission tomography imaging in tumor-bearing mice. European Journal of Pharmaceutical Sciences, 2021, 166, 105964.	4.0	7
89	PET Imaging of Adenosine Receptors in Diseases. Current Topics in Medicinal Chemistry, 2019, 19, 1445-1463.	2.1	7
90	Proteomic profiling of isogenic primary and metastatic medulloblastoma cell lines reveals differential expression of key metastatic factors. Journal of Proteomics, 2017, 160, 55-63	2.4	6

#	Article	IF	CITATIONS
91	A molecular imaging biosensor detects in vivo protein folding and misfolding. Journal of Molecular Medicine, 2016, 94, 799-808.	3.9	5
92	Legumain correlates with neuroblastoma differentiation and can be used in prodrug design. Chemical Biology and Drug Design, 2018, 91, 534-544.	3.2	5
93	Exploring Solvent Effects in the Radiosynthesis of <sup>18</sup> F-Labeled Thymidine Analogues toward Clinical Translation for Positron Emission Tomography Imaging. ACS Pharmacology and Translational Science, 2021, 4, 266-275.	4.9	5
94	Preclinical evaluation of a 64Cu-labeled disintegrin for PET imaging of prostate cancer. Amino Acids, 2019, 51, 1569-1575.	2.7	4
95	15,16-dihydrotanshinone I inhibits EOMA cells proliferation by interfering in posttranscriptional processing of hypoxia-inducible factor 1. International Journal of Medical Sciences, 2021, 18, 3214-3223.	2.5	2
96	Efficient multicistronic co-expression of hNIS and hTPO in prostate cancer cells for nonthyroidal tumor radioiodine therapy. American Journal of Nuclear Medicine and Molecular Imaging, 2012, 2, 483-98.	1.0	2
97	Crystal structure of 2-(2'-hydroxyphenyl)-6-tributylstannyl-4-(3H )-quinazolinone and 2-(2'-hydroxyphenyl)-6-iodo-4-(3H)-quinazolinone. Crystal Research and Technology, 2006, 41, 622-627.	1.3	1
98	In Vivo Tumor Angiogenesis Imaging Using Peptide-Based Near-Infrared Fluorescent Probes. Methods in Molecular Biology, 2016, 1444, 73-84.	0.9	1
99	[ <sup>18</sup> F]FMAU for PET imaging in breast cancer patients Journal of Clinical Oncology, 2015, 33, 11056-11056.	1.6	1
100	Effect of Androgen on Normal Biodistribution of [18F]-2'- Fluoro-5-methyl-1-beta-D-arabinofuranosyluracil (18F-FMAU) in Athymic Non-tumor-bearing Male Mice. Anticancer Research, 2017, 37, 475-480.	1.1	1
101	PET and SPECT Imaging of Tumor Vasculature. , 2012, , 341-371.		0